

CrystEngComm

Accepted Manuscript



This is an *Accepted Manuscript*, which has been through the Royal Society of Chemistry peer review process and has been accepted for publication.

Accepted Manuscripts are published online shortly after acceptance, before technical editing, formatting and proof reading. Using this free service, authors can make their results available to the community, in citable form, before we publish the edited article. We will replace this *Accepted Manuscript* with the edited and formatted *Advance Article* as soon as it is available.

You can find more information about *Accepted Manuscripts* in the [Information for Authors](#).

Please note that technical editing may introduce minor changes to the text and/or graphics, which may alter content. The journal's standard [Terms & Conditions](#) and the [Ethical guidelines](#) still apply. In no event shall the Royal Society of Chemistry be held responsible for any errors or omissions in this *Accepted Manuscript* or any consequences arising from the use of any information it contains.



Molecular salts of propranolol with dicarboxylic acids: Diversity of stoichiometry, supramolecular structures and physicochemical properties

Received 00th July 2015,
Accepted 00th January 2015

DOI: 10.1039/x0xx00000x

D. Stepanovs,^{a,b} M. Jure,^b A. Yanichev,^a S. Belyakov,^a and A. Mishnev^{a,b}

www.rsc.org/

Crystallization of the drug propranolol with dicarboxylic acids yielded stable crystalline molecular salts with oxalic and fumaric acids in molar ratios of 1:1 and 2:1, with maleic acid in the molar ratio of 1:1 only. The melting points of the salts obtained were roughly twice the melting point of pure propranolol, while aqueous solubility was significantly higher in comparison to propranolol base.

The majority of active pharmaceutical ingredients (API) show unwanted physicochemical properties that pose serious problems for clinical development and can lead to late stage drug failure.^{1,2} Improving the solubility and bioavailability of poorly water soluble drugs is a difficult challenge for pharmaceutical developers.³ However, highly soluble drugs are unsuitable for oral extended-release formulations; therefore, various approaches have been applied to resolve this issue, including polymer-based monolithic matrix tablets.⁴ Crystal engineering is a widely used approach that allows the construction of crystal forms of API with improved physicochemical properties.^{5–11} These crystals may appear in the form of molecular salts or cocrystals, but the term cocrystal is not currently well-defined.¹² According to U.S. FDA cocrystals are crystalline materials composed of two or more molecules within the same crystal lattice.¹³ However, the more restrictive definition have been proposed by scientific community: cocrystals are solids that are crystalline single phase materials composed of two or more different molecular/or ionic compounds generally in a stoichiometric ratio which are neither solvates nor simple salts.¹⁴ Both molecular salts and cocrystals are aimed at the improvement of pharmaceutical development, primarily the solubility and stability of API.¹⁵ Solubility is an important property that can affect the dissolution rate and, consequently, bioavailability.^{5,6} Solubility is closely related to the compound thermal behaviour. However, this dependence is not linear, because of a significant contribution of solvation effect.^{16,17} Strong correlations between the melting points of cofomer (counter ion) and multi-component pharmaceutical crystals (MCPC) have been reported in the literature.^{18,19} Disclosure

of such correlations would provide simple rules for the rational choice of cofomers in the design of MCPC with desirable thermal properties. The present study describes the design, preparation and selected physicochemical properties of propranolol (**pro**) pharmaceutical molecular salts with selected carboxylic acids (**Scheme 1**). The (**pro**) is a non-toxic,²⁰ nonselective β -adrenergic antagonist or simply β -blocker.^{21,22} It is used in the treatment or prevention of many disorders, including acute myocardial infarction, arrhythmias, angina pectoris, hypertension, hypertensive emergencies, hyperthyroidism, migraine, pheochromocytoma, menopause, and anxiety.^{23–25} Due to the poor solubility and relatively low melting point (92–93 °C) of (**pro**) base, the API has been marketed as a hydrochloride salt (melting point 163–164 °C) and is available as injections, tablets, and capsules. The oral administrated form strength is 80–160 mg dose and available as extended-release capsules. Thus, a prolongation of the drug action has been achieved by modifying a formulation or dosage form.²⁶ An alternative method would be using less soluble crystalline forms of the API. In this study, the crystal engineering by means of preparing (**pro**) molecular salts has been employed to obtain crystal forms with lower aqueous solubility. It is well known that solubility and other physicochemical properties are determined by crystal structural parameters, therefore crystal engineering is the key approach to design supramolecular structures with desired properties of API. Dicarboxylic acids are a popular cofomer choice for cocrystal engineering, and since these compounds are multi-ionizable, products with different stoichiometry can be obtained.^{27,28} They are most widely used to address the issue of solubility of an API. Cocrystallization of antibiotic API ciprofloxacin with maleic, fumaric, and adipic acids in stoichiometry 1:1 leads to formation of molecular salt with 7–33 fold enhanced solubility with respect to pure API.²⁹ The same API forms molecular salt with succinic acid with different stoichiometry (2:1 and 1:1); both salts show altered thermal behaviour and enhanced solubility with respect to pure ciprofloxacin and ciprofloxacin hydrochloride.²⁷ Antiviral API adefovir dipivoxil forms cocrystals with succinic and suberic acids (stoichiometry 2:1 and 1:1 respectively). Both cocrystals showed increased solubility at temperatures below 45 °C and enhanced thermal stability.²⁸ Antitumor drug temozolamide undergoes spontaneous degradation under normal conditions in aqueous medium with pH > 7. It readily forms cocrystals with carboxylic acids. Temozolamide cocrystals with oxalic acid (2:1) and

^a Latvian Institute of Organic Synthesis, 21 Aizkraukles street, Riga, LV-1006, Latvia

^b Faculty of Material Science and Applied Chemistry, Riga Technical University, 3 Paula Valdena street, Riga, LV-1007, Latvia.

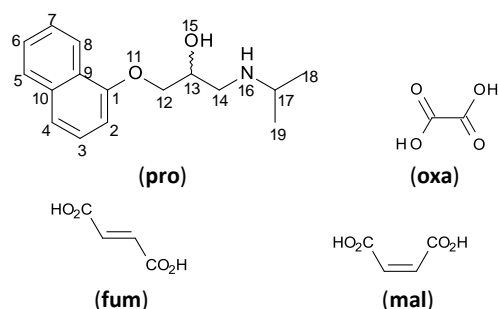
† Footnotes relating to the title and/or authors should appear here.

Electronic Supplementary Information (ESI) available: [experimental data, ORTEP drawings and CIF files]. See DOI: 10.1039/x0xx00000x

COMMUNICATION

CrystEngComm

succinic acid (2:1) showed enhanced stability with no signs of decomposition for up to one year.³⁰



Scheme 1. The structures and abbreviations of compounds used in this study. Atom-numbering scheme corresponds to those in crystal structures

The **(pro)** base has been obtained from a hydrochloride form.† The **(pro)** molecular salts with selected dicarboxylic acids have been prepared by treating dicarboxylic acid with **(pro)** base.§ The **(pro)** hydrogen oxalate, oxalate, oxalate methanol solvate, hydrogen fumarate, fumarate fumaric acid cocrystal, and hydrogen maleate have been obtained. The formation of molecular salts in the solid state has been proved by powder and single crystal X-ray diffraction (see **ESI S1-S5**), while in-solution formation was observed by nuclear magnetic resonance (NMR) (NMR ¹H spectra of salts show the changes in chemical shifts in respect to those on the pure **(pro)** spectrum). Signals of neighbouring protons are significantly shielded (chemical shifts are given in **ESI S6**). Selected crystal data as well as experimental and refinement parameters for **(pro)** structures are summarized in **ESI S3**.§§ Propranolol oxalate methanol solvate (2:1:0.9) contained the prohibited methanol molecule and was therefore excluded from further investigations after the single crystal structure was solved.

The *PXRD* patterns of the new **(pro)** molecular salts are depicted in **Figures 1-3** in comparison with the *PXRD* patterns of the initial compounds. The powder patterns of the products show no reflections from starting compounds, indicating complete reactions.

There are six new crystal structures of molecular salts reported in this work. In all structures **(pro)** cations and anions from dicarboxylic acids are present. H-atoms bonded to N atoms in the four compounds **(pro)⁺(fum)⁻** 1:1, **(pro)⁺(fum)⁻** 2:1, **(pro)⁺(mal)⁻**, and **(pro)⁺(oxa)⁻** 1:1 were refined isotropically. Also that H-atoms bonded to O atoms in the three compounds **(pro)⁺(fum)⁻** 1:1, **(pro)⁺(mal)⁻**, and **(pro)⁺(oxa)⁻** 1:1 were refined isotropically. The acid salt **(pro)** hydrogen oxalate is formed when **(pro)** and **(oxa)** is in stoichiometry 1:1. **Figure 4** illustrates fragments of the crystal structure of **(pro)⁺(oxa)⁻** 1:1 (ORTEP drawing of asymmetric units with thermal ellipsoids and atom-numbering schemes followed in the text for all structures depicted in **ESI S4**).

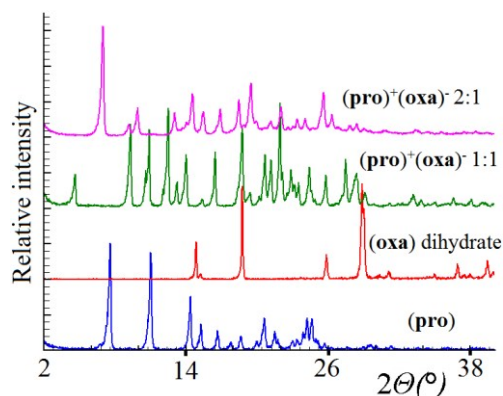


Figure 1. Experimental *PXRD* patterns of **(pro)⁺(oxa)⁻** 1:1 and 2:1 in comparison with pure compounds

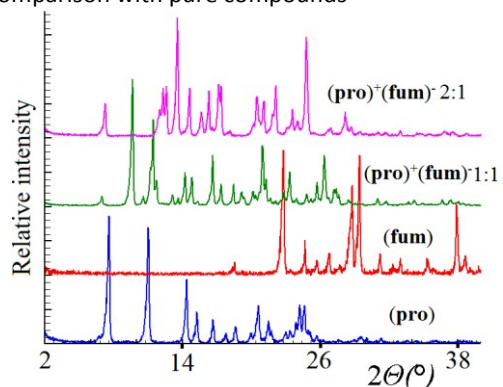


Figure 2. Experimental *PXRD* patterns of **(pro)⁺(fum)⁻** 1:1 and 2:1 in comparison with pure compounds

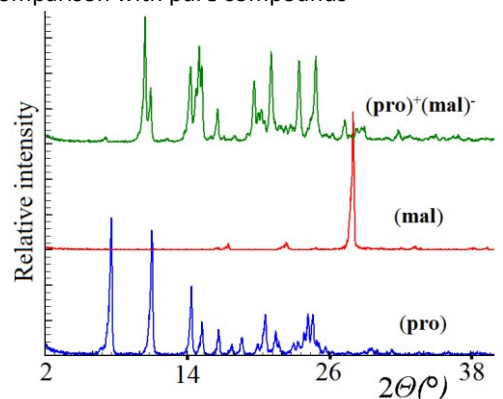


Figure 3. Experimental *PXRD* patterns of **(pro)⁺(mal)⁻** in comparison with pure compounds

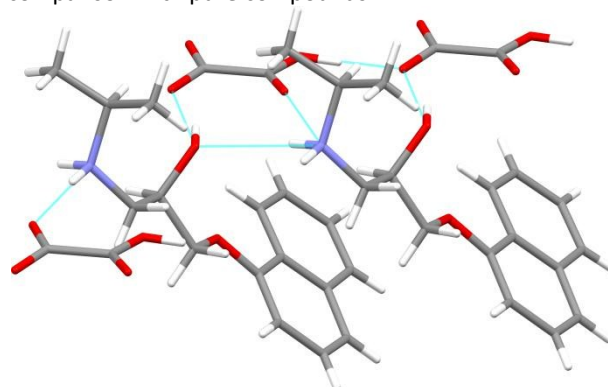


Figure 4. Mercury CSD 31.1³¹ crystal structure fragment of the **(pro)⁺(oxa)⁻** 1:1, hydrogen bonds are shown as dashed lines

Table 1 lists the torsion angles that characterize the conformation of the (**pro**)⁺ cation. The value of the O11–C12–C13–O15 (see Scheme 1 for atom numbering) torsion angle indicates that two C–O bonds are characterized by *gauche*-conformation relative to the C12–C13 bond. In (**pro**)⁺(**oxa**)⁻ 1:1, there are three acidic hydrogens and one hydrogen of the hydroxy group; all of these hydrogens take part in formation of strong hydrogen bonds. The parameters of these hydrogen bonds are given in **ESI S5**. The carboxyl group forms a very strong O–H...O hydrogen bond with O25 of another anion. By means of this bond, the anions generate chains along the monoclinic axis with graph-set **C(5)**.³² It should be noted that the crystal structure of (**pro**)⁺(**oxa**)⁻ 1:1 is chiral (space group *P2₁*), although the salt was obtained from racemic (**pro**) and achiral oxalic acid. This means that the substance of (**pro**)⁺(**oxa**)⁻ 1:1 is a racemic mixture of left and right enantiomorphous crystals. This provides an opportunity for obtaining of the enantiopure compounds manually.

Unlike (**pro**)⁺(**oxa**)⁻ 1:1, the salt of (**pro**)⁺(**oxa**)⁻ 2:1 (propranolol oxalate) crystallizes in the achiral space group *P2₁/c*. **Figure 5** shows the fragment of the crystal structure, where dashed lines represent hydrogen bonds. In this structure, the doubly charged oxalate anions are in special positions (centres of inversion), but the (**pro**)⁺ cations lie in general positions.

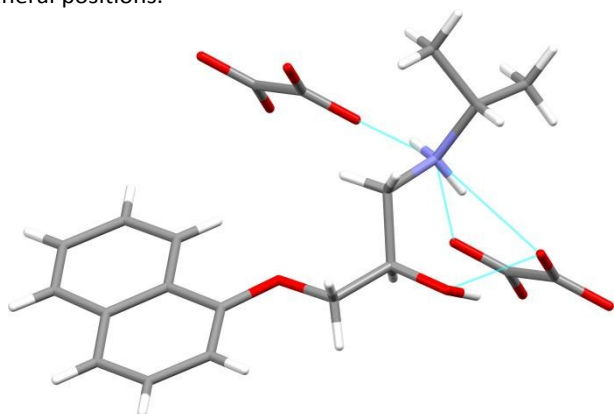


Figure 5. Mercury CSD 31.1³¹ crystal structure fragment of (**pro**)⁺(**oxa**)⁻ 2:1, hydrogen bonds are shown as dashed lines

The conformation of the cation differs from that in (**pro**)⁺(**oxa**)⁻ 1:1 (see **Table 1**). The intramolecular C–H...O hydrogen bond of (**pro**)⁺(**oxa**)⁻ 1:1 is not strong enough for conservation of the cation conformation. Two C–O bonds have *anti*-conformation relative to the C12–C13 bond. In the crystal structure of (**pro**)⁺(**oxa**)⁻ 2:1, hydrogens of OH and NH groups form strong intermolecular hydrogen bonds with the oxalate anions: the hydroxy group and N16–H16B are bonded with oxygens O21 and O20, respectively; N16–H16A forms bifurcated hydrogen bonds with oxygens (O20 and O21) of another oxalate anion.

The crystal structure of (**pro**)⁺(**oxa**)⁻ MeOH differs considerably from (**pro**)⁺(**oxa**)⁻ 2:1. The asymmetric unit of (**pro**)⁺(**oxa**)⁻ MeOH contains two (**pro**)⁺ cations, one oxalate anion and one methanol molecule (see **Figure 6**). In the crystal structure, the two cations are almost mirror symmetrical.

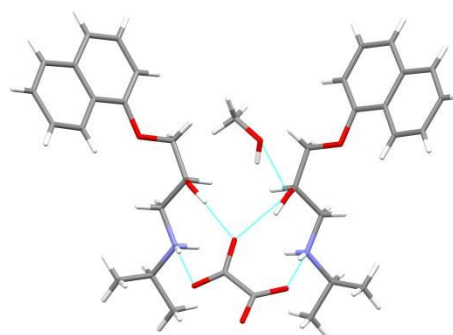


Figure 6. Mercury CSD 31.1³¹ crystal structure fragment of (**pro**)⁺(**oxa**)⁻ MeOH, only selected hydrogen bonds are shown as dashed lines for clarity

It should be noted that the oxalate anions are not planar in the crystal structure of (**pro**)⁺(**oxa**)⁻ MeOH: the value of *t*. O21–O22–O23–O24 torsion angle is 25.0(4)°.

Figure 7 shows the fragment of the (**pro**)⁺(**fum**)⁻ 2:1 crystal structure. In the cation structure, two C–O bonds are characterized both by *gauche*- and *anti*-conformations relative to the C12–C13 bond. The crystals (**pro**)⁺(**fum**)⁻ 2:1 are disordered, and the values of the occupation *g*-factor for disordered oxygen atoms (O15 and O15') are equal 0.5 (see **Figure 7**). The asymmetric unit has a (**pro**)⁺ cation in a general position and a one half fumarate ion, lying about an inversion centre. Unlike the (**pro**)⁺(**oxa**)⁻ structures in (**pro**)⁺(**fum**)⁻ 2:1, there is a weak π - π stacking interaction between pairs of inversion-related naphthyl rings; the distance between the naphthyl planes is 3.541(3) Å.

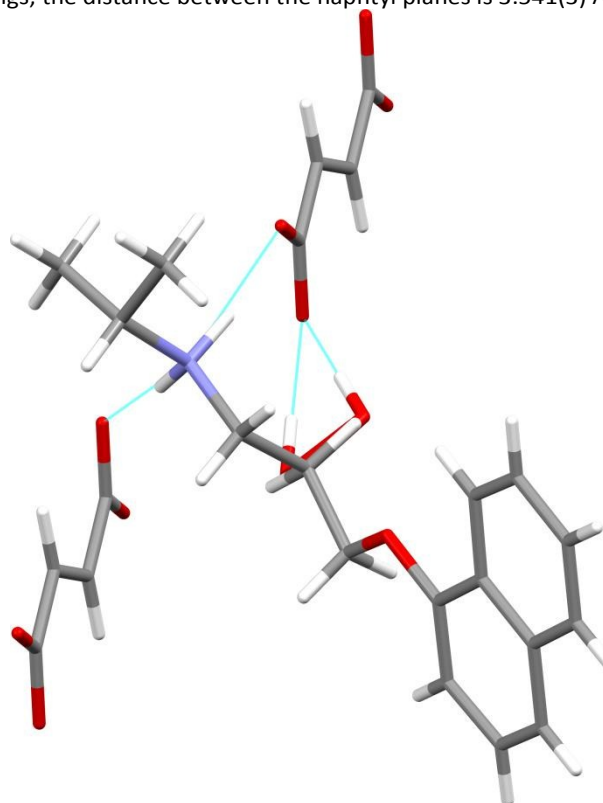


Figure 7. Mercury CSD 31.1³¹ crystal structure fragment of (**pro**)⁺(**fum**)⁻ 2:1, hydrogen bonds are shown as dashed lines

The crystal structure of $(\text{pro})^+(\text{fum})^-$ 1:1 (Figure 8) represents a propranolol fumarate and fumaric acid cocrystal.

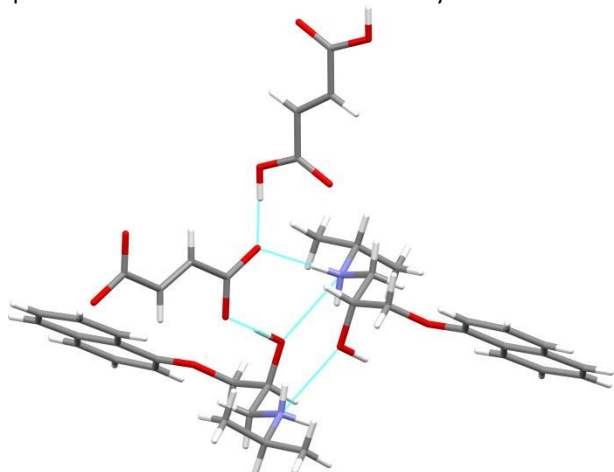


Figure 8. Mercury CSD 31.1³¹ crystal structure fragment of $(\text{pro})^+(\text{fum})^-$ 1:1, hydrogen bonds are shown as dashed lines

The asymmetric unit has a propranolol moiety in a general position as well as a one half fumaric acid molecule and a one half fumarate ion, each lying about independent inversion centres.

Unlike oxalic and fumaric acid, the maleic acid³³ is practically monoprotic. It gives salt with (pro) in stoichiometry 1:1 only. **Figure 9** shows a fragment of the crystal structure of $(\text{pro})^+(\text{mal})^-$. Both components lie on general positions with no crystallographically-imposed symmetry. The O15–H15, N16–H16A and N16–H16B groups form strong hydrogen bonds with three maleate anions (see **ESI S5**).

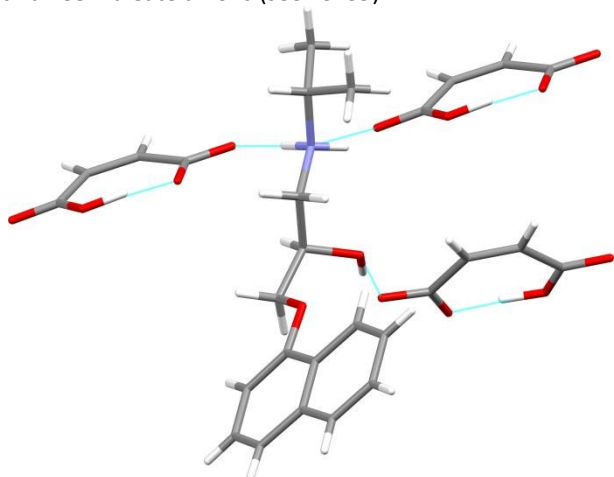


Figure 9. Mercury CSD 31.1³¹ structure fragment of the structure of $(\text{pro})^+(\text{mal})^-$, hydrogen bonds are shown as dashed lines

In the crystal structure, the frameworks are formed with the help of the strong hydrogen bonds (see **ESI S5**). These frames are parallel to the crystallographic plane (0 0 1).

As has been demonstrated, dicarboxylic acids possess two acidic protons, so carboxylates as well as hydrogen carboxylates can be formed. From a toxicological perspective, these different salt forms – carboxylates and hydrogen

carboxylates – should not behave differently, as in any case the anion which is part of API has to be dissolved and therefore a fast equilibrium between the different ionization states exists. This equilibrium will only depend on pH in the respective segment of gastrointestinal tract. However, especially for drugs that must be given in high doses, the usage of carboxylates instead of hydrogen carboxylates can be useful, as this will introduce only half as much inactive components from the counterion into the API.

Melting points of molecular salts were determined using DTA (see **ESI S7**). Also molecular salts have been tested with elemental analysis (**ESI S8**). All of the solubility experiments were carried out in an aqueous medium at 24 hours (see also **ESI S9**). It is assumed that after 24 hours, dissolved and undissolved particles are in dynamic equilibrium. Examination of the solid phase by PXRD (see **ESI S9**) after solubility experiments revealed that precipitates contained only initial molecular salts. Among all binary systems, $(\text{pro})^+(\text{fum})^-$ 1:1 and $(\text{pro})^+(\text{fum})^-$ 2:1 showed the lowest solubility of 5.2 and 6.7 mg/ml each, which is attributed to the low solubility of fumaric acid. As expected, $(\text{pro})^+(\text{mal})^-$ exhibited the highest solubility among other salts because of the high solubility of the maleic acid. The advantages of carboxylates in comparison to hydrogen carboxylates are higher solubility and the introduction of half as much acid into API.

Generally, the (pro) molecular salts with dicarboxylic acids exhibited a 40–85 fold increase in the aqueous solubility of (pro) compared to (pro) base and a 25–54 fold decrease compared to highly soluble (pro) hydrochloride (see **Table 1**). A relatively low correlation has been found between solubility and the melting points of salts. In addition, a better correlation is achieved if we consider melting onset as the function of solubility S (not $\log S$)⁶ (see **Figure 10**). It should be underlined that relatively low value of the correlation coefficient indicates a non-linear dependence. As expected, the doubly charged molecular salts have higher melting points in comparison to corresponding monocharged salts.

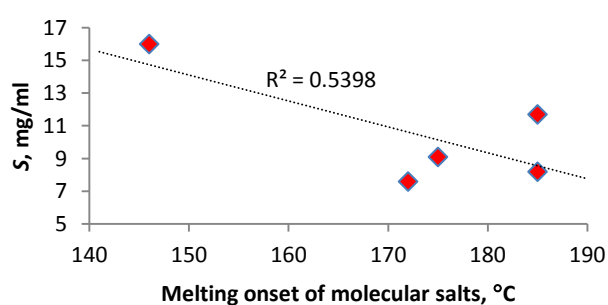


Figure 10. Solubility as a function of molecular salt melting point

We have demonstrated that the selection and crystal engineering of molecular salts of target molecule leads to altered physicochemical properties, especially aqueous solubility. Further studies should include the determination of dissolution rates.

Conclusions

Propranolol hydrogen oxalate, oxalate, oxalate methanol solvate, hydrogen fumarate, fumarate fumaric acid cocrystal, and hydrogen maleate have been obtained and characterized by X-ray single crystal and powder diffraction, DTA, and other analytical techniques. Propranolol molecular salts exhibit a 40–85 fold increase in the aqueous solubility of propranolol compared to propranolol base and a 24–54 fold decrease compared to highly soluble propranolol hydrochloride. The melting point of pure propranolol has been considerably enhanced in the salt products. The results obtained so far show promising properties of (**pro**) salts for the preparation of extended-release formulations.

Notes and references

† The (**pro**) base was prepared from hydrochloride salt. One gram of the (**pro**) hydrochloride was dissolved in 50 ml of distilled water and saturated NaCO₃ aqueous solution was added up to pH 7.5. The (**pro**) base was precipitated out and then extracted using diethyl ether. The extraction process was completed several times using 50 ml of diethyl ether. Crystalline (**pro**) base was obtained after the solvent evaporated. The crystal structure of the (**pro**) base has been reported in literature.²⁴

§ Molecular salts formed when the (**pro**) base (50 mg, 0.19 mmol) and dicarboxylic acid in 1:1 and 2:1 molar ratios were dissolved in the corresponding solvent and left for solvent evaporation for several days. Single crystals suitable for X-ray analysis were collected during these experiments.

§§ Crystal data for (**pro**)⁺(**oxa**)⁻ 1:1: (C₁₆H₂₂NO₂)⁺·(C₂H₂O₄)⁻ (*M* = 349.37), monoclinic, *P*2₁, *a* = 8.1696(3), *b* = 5.6053(2), *c* = 18.9321(9) Å, *β* = 98.820(2)°, *V* = 856.71(6) Å³, *T* = 173(2) K, *Z* = 2, *μ*(MoKα) = 0.102 mm⁻¹, 4766 reflections measured, 3202 independent reflections, *R*_{1(obs)} = 0.067, *wR*_{1(obs)} = 0.108, *R*_{1(all)} = 0.115, *wR*_{1(all)} = 0.124, *S* = 1.01; (**pro**)⁺(**oxa**)⁻ 2:1: (C₁₆H₂₂NO₂)⁺·0.5(C₂O₄)²⁻ (*M* = 304.36), monoclinic, *P*2₁/*c*, *a* = 12.9928(6), *b* = 6.4517(3), *c* = 19.8420(13) Å, *β* = 106.600(2)°, *V* = 1593.95(9) Å³, *T* = 173(2) K, *Z* = 4, *μ*(MoKα) = 0.090 mm⁻¹, 6582 reflections measured, 3782 independent reflections (*R*_{int} = 0.134), *R*_{1(obs)} = 0.162, *wR*_{1(obs)} = 0.399, *R*_{1(all)} = 0.277, *wR*_{1(all)} = 0.453, *S* = 1.05; (**pro**)⁺(**oxa**)⁻ MeOH: 2(C₁₆H₂₂NO₂)⁺·(C₂O₄)²⁻·0.9(CH₄O) (*M* = 637.55), orthorhombic, *Pbn*2₁, *a* = 10.7741(2), *b* = 11.3507(2), *c* = 28.2413(6) Å, *V* = 3453.73(11) Å³, *T* = 173(2) K, *Z* = 4, *μ*(MoKα) = 0.088 mm⁻¹, 12030 reflections measured, 12030 independent reflections, *R*_{1(obs)} = 0.079, *wR*_{1(obs)} = 0.121, *R*_{1(all)} = 0.236, *wR*_{1(all)} = 0.160, *S* = 0.99; (**pro**)⁺(**fum**)⁻ 1:1: (C₁₆H₂₂NO₂)⁺·0.5(C₄H₄O₄)⁻·0.5(C₄H₂O₄)²⁻ (*M* = 375.41), triclinic, *P*1̄, *a* = 8.6157(2), *b* = 9.9155(2), *c* = 13.1345(4) Å, *α* = 97.391(1)°, *β* = 102.240(1)°, *γ* = 109.899(1)°, *V* = 1006.17(4) Å³, *T* = 173(2) K, *Z* = 2, *μ*(MoKα) = 0.091 mm⁻¹, 6668 reflections measured, 4597 independent reflections (*R*_{int} = 0.018), *R*_{1(obs)} = 0.048, *wR*_{1(obs)} = 0.121, *R*_{1(all)} = 0.056, *wR*_{1(all)} = 0.127, *S* = 1.04; (**pro**)⁺(**fum**)⁻ 2:1: (C₁₆H₂₂NO₂)⁺·0.5(C₄H₂O₄)²⁻ (*M* = 317.37), triclinic, *P*1̄, *a* = 7.7989(3), *b* = 9.1669(4), *c* = 12.4724(6) Å, *α* = 89.470(2)°, *β* = 75.754(2)°, *γ* = 76.412(3)°, *V* = 836.95(6) Å³, *T* = 173(2) K, *Z* = 2, *μ*(MoKα) = 0.088 mm⁻¹, 5428 reflections measured, 3805 independent reflections (*R*_{int} = 0.021), *R*_{1(obs)} =

0.052, *wR*_{1(obs)} = 0.115, *R*_{1(all)} = 0.071, *wR*_{1(all)} = 0.126, *S* = 1.04; (**pro**)⁺(**mal**)⁻: (C₁₆H₂₂NO₂)⁺·(C₄H₃O₄)⁻ (*M* = 375.41), monoclinic, *P*2₁/*n*, *a* = 9.2010(3), *b* = 8.7153(3), *c* = 24.7710(11) Å, *β* = 94.618(1)°, *V* = 1979.93(13) Å³, *T* = 173(2) K, *Z* = 4, *μ*(MoKα) = 0.093 mm⁻¹, 11927 reflections measured, 4491 independent reflections (*R*_{int} = 0.148), *R*_{1(obs)} = 0.083, *wR*_{1(obs)} = 0.118, *R*_{1(all)} = 0.238, *wR*_{1(all)} = 0.153, *S* = 0.98.

- (1) Kola, I.; Landis, J. *Nat. Rev. Drug Discov.* **2004**, *3*, 711–716.
- (2) Chemburkar, S. R.; Bauer, J.; Deming, K.; Spiwek, H.; Patel, K.; Morris, J.; Henry, R.; Spanton, S.; Dziki, W.; Porter, W.; Quick, J.; Bauer, P.; Donaubaue, J.; Narayanan, B. A.; Soldani, M.; Riley, D.; McFarland, K. *Org. Process Res. Dev.* **2000**, *4*, 413–417.
- (3) Mittapalli, S.; Mannava, M. K. C.; Khandavilli, U. B. R.; Al S.; Nangia, A. *Cryst. Growth Des.* **2015**, *15*, 2493–2504.
- (4) Shao, Y.; Li, L.; Gu, X.; Wang, L.; Mao, S. *Asian J. Pharm. Sci.* **2015**, *10*, 24–30.
- (5) Batisai, E.; Ayamine, A.; Kilinkissa, O. E. Y.; Báthori, N. B. *CrystEngComm* **2014**, *16*, 9992–9998.
- (6) Schultheiss, N.; Newman, A. *Cryst. Growth Des.* **2009**, *9*, 2950–2967.
- (7) Žegarac, M.; Lekšić, E.; Šket, P.; Plavec, J.; Devčić, M.; Bogdanović, M.; Bučar, D.-K.; Dumić, M.; Meštrović, E. *CrystEngComm* **2014**, *16*, 32.
- (8) Aitipamula, S.; Wong, A. B. H.; Chow, P. S.; Tan, R. B. H. *Cryst. Growth Des.* **2014**, *14*, 2542–2556.
- (9) Sheikh, A. Y.; Rahim, S. A.; Hammond, R. B.; Roberts, K. J. *CrystEngComm* **2009**, *11*, 501.
- (10) Stepanovs, D.; Jure, M.; Kuleshova, L. N.; Hofmann, D. W. M.; Mishnev, A. *Cryst. Growth Des.* **2015**, *15*, 3652–3660.
- (11) Aakeröy, C. B.; Champness, N. R.; Janiak, C. *CrystEngComm* **2010**, *12*, 22.
- (12) Aakeröy, C. B.; Salmon, D. J. *CrystEngComm* **2005**, *7*, 439.
- (13) Administration, U. S. F. and D. Regulatory Classification of Pharmaceutical Co-Crystals. <http://www.fda.gov/downloads/drugs/guidancecompliance/regulatoryinformation/guidances/ucm281764.pdf>.
- (14) Aitipamula, S.; Banerjee, R.; Bansal, A. K.; Biradha, K.; Cheney, M. L.; Choudhury, A. R.; Desiraju, G. R.; Dikundwar, A. G.; Dubey, R.; Duggirala, N.; Ghogale, P. P.; Ghosh, S.; Goswami, P. K.; Goud, N. R.; Jetli, R. R. K. R.; Karpinski, P.; Kaushik, P.; Kumar, D.; Kumar, V.; Moulton, B.; Mukherjee, A.; Mukherjee, G.; Myerson, A. S.; Puri, V.; Ramanan, A.; Rajamannar, T.; Reddy, C. M.; Rodriguez-Hornedo, N.; Rogers, R. D.; Row, T. N. G.; Sanphui, P.; Shan, N.; Shete, G.; Singh, A.; Sun, C. C.; Swift, J. A.; Thaimattam, R.; Thakur, T. S.; Kumar Thaper, R.; Thomas, S. P.; Tothadi, S.; Vangala, V. R.; Variankaval, N.; Vishweshwar, P.; Weyna, D. R.; Zaworotko, M. J. *Cryst. Growth Des.* **2012**, *12*, 2147–2152.
- (15) Good, D. J.; Rodríguez-Hornedo, N. *Cryst. Growth Des.* **2009**, *9*, 2252–2264.
- (16) Genheden, S.; Mikulskis, P.; Hu, L.; Kongsted, J.; Söderhjelm, P.; Ryde, U. *J. Am. Chem. Soc.* **2011**, *133*, 13081–13092.
- (17) Choi, H.; Kang, H.; Park, H. *J. Cheminform.* **2013**, *5*, 8.
- (18) Stanton, M. K.; Bak, A. *Cryst. Growth Des.* **2008**, *8*, 3856–3862.

- (19) Aakeröy, C. B.; Hussain, I.; Desper, J. *Cryst. Growth Des.* **2006**, *6*, 474–480.
- (20) Franklin, S.; Balasubramanian, T.; Nehru, K.; Kim, Y. *J. Mol. Struct.* **2009**, *927*, 121–125.
- (21) Gladstone, G. R.; Hordof, A.; Gersony, W. M. *J. Pediatr.* **1975**, *86*, 962–964.
- (22) Holroyd, K. A.; Penzien, D. B.; Cordingley, G. E. *Headache J. Head Face Pain* **1991**, *31*, 333–340.
- (23) Bredikhin, A. A.; Bredikhina, Z. A.; Gubaidullin, A. T.; Krivolapov, D. B.; Litvinov, I. A. *Mendeleev Commun.* **2004**, *14*, 268–270.
- (24) Ammon, H. L.; Howe, D. B.; Erhardt, W. D.; Balsamo, A.; Macchia, B.; Macchia, F.; Keefe, W. E. *Acta Crystallogr. Sect. B Struct. Crystallogr. Cryst. Chem.* **1977**, *33*, 21–29.
- (25) Gadret, M.; Goursole, M.; Leger, J. M.; Colleter, J. C. *Acta Crystallogr. Sect. B Struct. Crystallogr. Cryst. Chem.* **1975**, *31*, 1938–1942.
- (26) Sawayanagi, Y.; Nambu, N.; Nagai, T. *Chem. Pharm. Bull. (Tokyo)*. **1982**, *30*, 4213–4215.
- (27) Paluch, K. J.; McCabe, T.; Müller-Bunz, H.; Corrigan, O. I.; Healy, A. M.; Tajber, L. *Mol. Pharm.* **2013**, *10*, 3640–3654.
- (28) Jung, S.; Lee, J.; Kim, I. W. *J. Cryst. Growth* **2013**, *373*, 59–63.
- (29) Kovács, K.; Stampf, G.; Klebovich, I.; Antal, I.; Ludányi, K. *Eur. J. Pharm. Sci.* **2009**, *36*, 352–358.
- (30) Babu, N. J.; Sanphui, P.; Nangia, A. *Chem. - An Asian J.* **2012**, *7*, 2274–2285.
- (31) Macrae, C. F.; Bruno, I. J.; Chisholm, J. A.; Edgington, P. R.; McCabe, P.; Pidcock, E.; Rodriguez-Monge, L.; Taylor, R.; van de Streek, J.; Wood, P. A. *J. Appl. Crystallogr.* **2008**, *41*, 466–470.
- (32) Bernstein, J.; Davis, R. E.; Shimoni, L.; Chang, N.-L. *Angew. Chemie Int. Ed. English* **1995**, *34*, 1555–1573.
- (33) Day, G. M.; Trask, A. V.; Motherwell, W. D. S.; Jones, W. *Chem. Commun. (Camb)*. **2006**, 54–56.
- (34) Suzuki, Y.; Muraishi, K.; Matsuki, K. *Thermochim. Acta* **1992**, *211*, 171–180.

Table 1 Values of selected torsion angles τ (in deg.) of (pro) cations in the studied crystal structures

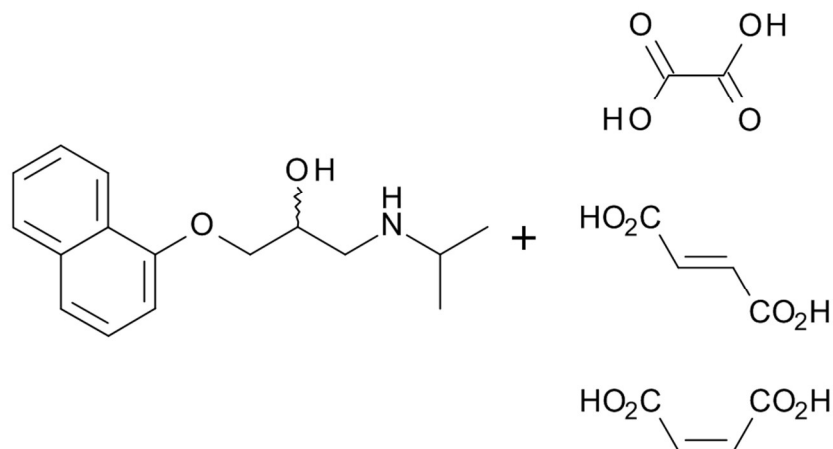
Torsion angle	Compound					
	(pro) ⁺ (oxa) ⁻ 1:1	(pro) ⁺ (oxa) ⁻ 2:1	(pro) ⁺ (oxa) ⁻ MeOH for cations A and B	(pro) ⁺ (fum) ⁻ 1:1	(pro) ⁺ (fum) ⁻ 2:1	(pro) ⁺ (mal) ⁻
C2–C1–O11–C12	4.7(4)	-2.6(12)	7.6(5); -7.5(5)	-5.2(2)	3.3(2)	-4.3(4)
C1–O11–C12–C13	168.5(2)	174.9(7)	173.0(3); -175.3(3)	-171.2(1)	179.3(1)	-175.5(2)
O11–C12–C13–C14	178.8(2)	64.9(9)	-58.0(4); 59.1(4)	-58.8(2)	-56.6(1)	-54.7(3)
O11–C12–C13–O15	-62.7(3)	-173.0(6)	64.2(4); -63.1(4)	166.8(2); 79.2(2) [*]	67.9(1)	64.6(4)
C12–C13–C14–N16	170.2(2)	-166.0(6)	175.3(3); -173.0(3)	167.8(1)	174.2(1)	165.9(3)
C13–C14–N16–C17	-67.6(3)	-132.3(7)	-179.5(3); -178.6(3)	-178.3(1)	178.2(1)	179.3(3)
C14–N16–C17–C18	177.0(2)	174.8(7)	166.5(4); -167.9(4)	-166.5(1)	-163.6(1)	-170.2(3)
C14–N16–C17–C19	-61.0(3)	-61.8(10)	-70.3(4); 68.9(4)	70.8(2)	71.6(2)	65.1(4)

Table 2 Physicochemical properties of (pro) and (pro) molecular salt

Salt	Melting point (°C)			Water solubility, mg/ml			
	(pro)	acid ³⁴	salt	(pro)	acid	salt	(pro) ^{**}
(pro)-HCl	92-93	-	163-164	0.13 ± 0.06	-	319.8 ± 6.2	280.4 ± 5.4
(pro) ⁺ (oxa) ⁻ 1:1		190	175-182		98	9.1 ± 0.01	6.8 ± 0.01
(pro) ⁺ (oxa) ⁻ 2:1		190	185-191		98	11.7 ± 0.2	10.0 ± 0.1
(pro) ⁺ (fum) ⁻ 1:1		282	172-175		7	7.6 ± 0.2	5.2 ± 0.1
(pro) ⁺ (fum) ⁻ 2:1		282	185-189		7	8.2 ± 0.2	6.7 ± 0.1
(pro) ⁺ (mal) ⁻		144	146-149		441	16.0 ± 0.4	11.0 ± 0.3

* In (pro)⁺(fum)⁻ 1:1 the O11–C12–C13–O15 torsion angle values are given for two disordered cations

** Concentration of (pro) in salt solution



Crystallization of the drug propranolol with dicarboxylic acids yielded molecular salts with oxalic and fumaric acids in molar ratios of 1:1 and 2:1, with maleic acid in the molar ratio of 1:1

100x57mm (300 x 300 DPI)